

Dielectronic recombination and stability of warm gas in AGN

Susmita Chakravorty¹*, Ajit K. Kembhavi¹*, Martin Elvis²*, Gary Ferland³*, N.R.Badnell⁴*

¹*IUCAA, Post Bag 4, Ganeshkhind, Pune 411 007, India;*

²*Harvard-Smithsonian Center for Astrophysics, Cambridge, MA 02138;*

³*Department of Physics and Astronomy, University of Kentucky, Lexington, KY 40506;*

⁴*Department of Physics, University of Strathclyde, Glasgow G4 0NG, UK.*

23 February 2019

ABSTRACT

Understanding the thermal equilibrium (stability) curve may offer insights into the nature of the warm absorbers often found in active galactic nuclei. Its shape is determined by factors like the spectrum of the ionizing continuum and the chemical composition of the gas. We find that the stability curves obtained under the same set of conditions, but using recently derived dielectronic recombination rates, give significantly different results, especially in the regions corresponding to warm absorbers, leading to different physical predictions. Using the current rates we find a larger probability of having thermally stable warm absorber at 10^5 K than previous predictions and also a greater possibility for its multiphase nature. The results obtained with the current dielectronic recombination rate coefficients are more reliable because the warm absorber models along the stability curve have computed coefficient values, whereas previous calculations relied on guessed averages for the same due to lack of available data.

Key words: quasars: absorption lines - galaxies : active - ISM - ISM: lines and bands - abundances - atoms

1 INTRODUCTION

Warm Absorbers are highly photoionised gas found along our line of sight to the continuum source of active galactic nuclei (AGN). Their signatures are a wealth of absorption lines and edges from highly ionized species, notably OVII, OVIII, FeXVII, NeX, CV and CVI in the soft X-ray (0.3-1.5 keV) spectra. The typical column density observed for the gas is $N_{\text{H}} \sim 10^{22 \pm 1} \text{ cm}^{-2}$ and the temperature T is estimated to be a few times 10^5 K. For many objects the warm absorber exists as a multiphase absorbing medium with all the phases in near pressure equilibrium (Morales, Fabian & Reynolds, 2000; Collinge et al. 2001; Kaastra et al. 2002; Krongold et al. 2003; Netzer et al. 2003; Krongold et al. 2005; Ashton et al. 2006).

Any stable photoionised gas will lie on the thermal equilibrium curve or ‘stability’ curve, in the temperature - pressure phase space, where heating balances cooling; this curve is often used to study the multiphase nature of the photoionised gas. The equilibrium depends on the shape of the ionizing continuum and the chemical abundance of the gas (Krolik, McKee & Tarter, 1981; Krolik & Kriss, 2001; Reynolds & Fabian, 1995 and Komossa & Mathur,

2001). We are investigating this dependences in details and will report elsewhere (Chakravorty et al. , to be submitted).

Over the past two decades the estimates of dielectronic recombination rate coefficients have improved. In this letter we show that these have affected the stability curves significantly which may lead to quite different physical models for the warm absorber gas. We conclude with a caution on the reliability of earlier results.

2 THE STABILITY CURVE

As is customary, we consider an optically thin, plane parallel slab of gas being photoionised by the central source of the AGN. In ionization equilibrium, photoionisation is balanced by recombinations. Thermal equilibrium is achieved when photoionisation and Compton heating are balanced by collisional cooling, recombination, line-excitation, bremsstrahlung and Compton cooling. The conditions under which these equilibriums are achieved depend on the shape of the continuum, metallicity of the gas, the density, the column density, and the ratio of the ionizing photon flux to the gas density. Following the convention of Tarter, Tucker & Salpeter (1969) we specify this ratio through an *ionization parameter* $\xi = L/nR^2$, where L is the luminosity of the source and n the number density of gas at a distance R from the center of the AGN.

We consider a sequence of models for a range of ionization parameters ξ , for optically thin gas having constant density of 10^9 cm^{-3} , being irradiated by a power-law ionizing continuum

* E-mail: susmita@iucaa.ernet.in (SC); akk@iucaa.ernet.in (AK); elvis@head.cfa.harvard.edu (MA); gary@pa.uky.edu (GF); badnell@phys.strath.ac.uk (NB)

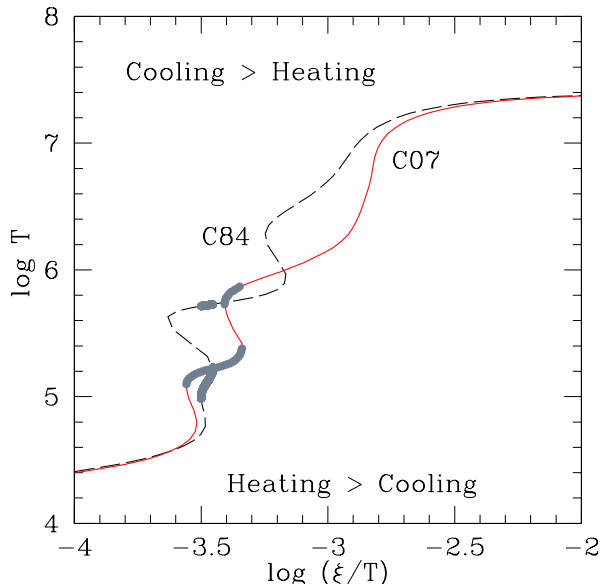


Figure 1. Stability curves generated by versions C07 and C84 of CLOUDY, for an optically thin gas with constant density 10^9 cm^{-3} , being ionized by a power-law continuum with photon index $\Gamma = 1.8$, extending from 13.6 eV to 40 keV. The gas, in both cases, is assumed to have *old Solar abundance* (see text). Regions of the plane where heating or cooling dominates are indicated. The curves are seen to differ significantly in the temperature range of $4.2 \leq \log T \leq 7.0$. Multiphase regions on the solid and dashed curve have been highlighted.

with photon index $\Gamma = 1.8$, so that $f(\nu) \sim \nu^{-(\Gamma-1)}$, and extending from 13.6 eV to 40 keV. The chemical composition of the gas (referred to as *old Solar abundance*) is due to Grevesse and Anders (1989) with extensions by Grevesse and Noels (1993). These parameter values (hereafter called the *standard set* of parameters) have been considered because that allows us to compare our results easily with earlier work.

Using version C07.02.01¹ (hereafter C07) of the photoionisation code CLOUDY (see Ferland et al. 1998 for a description), we plot the thermal stability curve which is shown as the solid curve (labeled C07) in Figure 1. ξ/T is proportional to p_{rad}/p , where p_{rad} is the radiation pressure and p the gas pressure; so an isobaric perturbation of a system in equilibrium is represented by a vertical displacement from the curve, and only changes the temperature. If the system being perturbed is located on a part of the curve with positive slope, which covers most of the curve, then a perturbation corresponding to an increase in temperature leads to cooling, while a decrease in temperature leads to heating of the gas. Such a gas is therefore thermally stable. But if the system is located on one of the few parts of the curve with negative slope, then it is thermally unstable because isobaric perturbations will lead to runaway heating or cooling.

3 COMPARISON WITH PREVIOUS WORK

Reynolds & Fabian (1995, hereafter RF95), have studied the stability curve for the warm absorber in MCG-6-30-15, using the standard set of parameters given above. We have reproduced their

Version	ξ_5	N_{phases}	$\Delta \log(\xi/T)$		$\Delta_M \log(\xi/T)$
			10^5 K	$\sim 10^6 \text{ K}$	
C84	45	2	0.05	0.47	0.05
C07	74	2	0.22	0.46	0.07

Table 1. Parameters for the warm absorber obtained using versions C84 and C07 of CLOUDY. The second column gives the value of the ionization parameter of the $\sim 10^5 \text{ K}$ stable warm absorber phase, the third column the number of discrete phases in the multiphase medium, the fourth and fifth columns the range of $\log(\xi/T)$ respectively for the $\sim 10^5 \text{ K}$ and $\sim 10^6 \text{ K}$ stable warm absorber phases and the sixth column the range of $\log(\xi/T)$ over which a multiphase medium is obtained.

curve, as given in Figure 3 of RF95, using version C84.12a (hereafter C84) of CLOUDY, which was the stable version between 1993 and 1996; this is shown as the dashed curve in Figure 1. The C84 and C07 curves match at high temperatures in the range $T > 10^{7.2} \text{ K}$, where Compton heating and cooling dominate. They also agree at low temperatures $T \lesssim 10^{4.5} \text{ K}$. However, the curves are significantly different in the intermediate temperature range $10^{4.5} \leq T \leq 10^{7.2} \text{ K}$, which is the region of interest for the warm absorbers and where recombination and line excitation are dominant cooling mechanisms.

A detailed comparison between the stable phases for warm absorbers predicted by the two different versions of CLOUDY is done in Table 1. The second column of the table shows that for an absorber at $T \sim 10^5 \text{ K}$, C84 predicts $\xi_5 \sim 45$, as compared to $\xi_5 \sim 74$ obtained from the C07 stability curve, where ξ_5 is defined to be the ionization parameter corresponding to the middle of the 10^5 K stable warm absorber phase. Both C84 and C07 predict two discrete phases of warm absorber at $\sim 10^5$ and $\sim 10^{5.7} \text{ K}$ which are in pressure equilibrium with each other and have been highlighted in Figure 1. The C07 curve continues to have stable thermal states at $\sim 10^6 \text{ K}$ which is not true in the C84 case. The range of $\log(\xi/T)$, over which the warm absorber exists are given in the fourth and fifth columns of respectively for the low and high temperature states. The extent of the 10^5 K phase in $\log(\xi/T)$ is about four times larger in C07, predicting greater probability of finding 10^5 K warm absorbers. In the sixth column we have compared the range $\Delta_M \log(\xi/T)$ where the warm absorber exhibits multiple phases. C07 predicts a 40% larger range and hence greater possibility of a multiphase warm absorber.

In order to isolate the atomic physics underlying the change in the stability curve, we have plotted the fractional variation of temperature $\Delta T/T_{\text{C07}} = (T_{\text{C84}} - T_{\text{C07}})/T_{\text{C07}}$, from one version to another, against $\log \xi$ in the top panel of Figure 2. We see that $\Delta T > 0$ for a major part of the range $1.0 < \log \xi < 4.5$, so that the gas is predicted to be cooler by C07. The cooling fractions (ΔC) of the major cooling agents and the heating fractions (ΔH) contributed by the principal heating agents using C07 are plotted against $\log \xi$ respectively in the middle and bottom panel of Figure 2. The ions which contribute significantly where $\Delta T/T_{\text{C07}} \gtrsim 0.5$, are He^{+1} , high ionization species of silicon (+10 and +11) and iron (+21, +22 and +23). In the same $\log \xi$ range, the principal heating agents are highly ionized species of oxygen (+6 and +7) and iron (+17 to +25).

To identify the ions which are responsible for $\Delta T/T_{\text{C07}} \gtrsim 50\%$, we compare their column densities predicted by C84 and C07. In the previous photoionisation calculations in this paper it

¹ <http://www.nublado.org/>

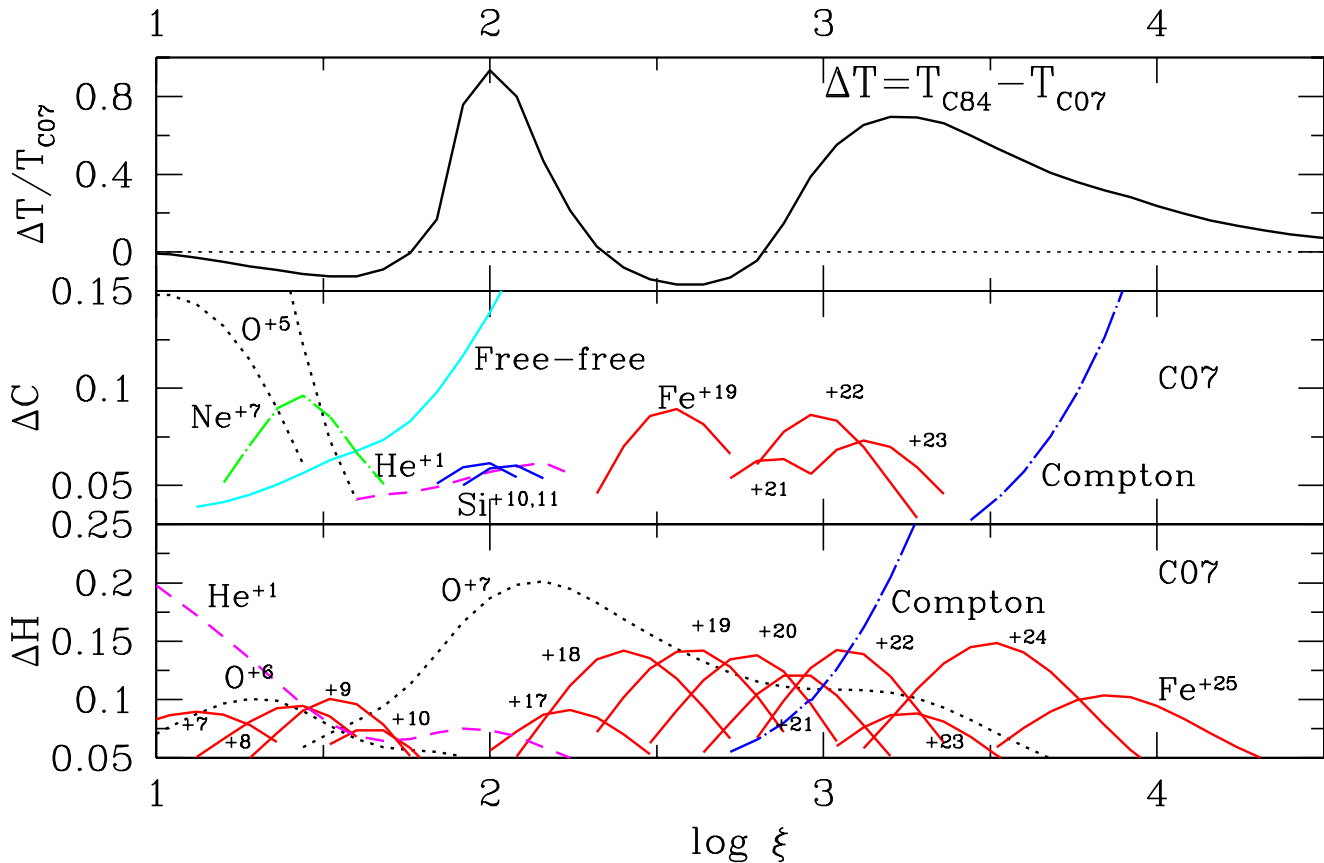


Figure 2. Top : The fractional change of temperature between the two versions C84 and C07 as a function of the ionization parameter. Middle : The cooling fraction (ΔC) for the major cooling agents as a function of $\log \xi$, using C07. He^{+1} and highly ionized species of silicon and iron play important roles. Bottom : The heating fraction (ΔH) contributed by the principle heating agents as a function of the ionization parameter, obtained using C07. Highly ionized species of oxygen like O^{+6} , O^{+7} , and various ions of iron like Fe^{+7} to Fe^{+10} and Fe^{+17} to Fe^{+25} are the key ingredients that are responsible for heating the gas in the range $1.0 < \log \xi < 4.5$.

was sufficient to use one zone models for optically thin gas. However, to calculate and compare the column densities of the ions over the range $1.0 < \log \xi < 4.5$, we chose to specify the gas to have total hydrogen column density $N_{\text{H}} = 10^{22} \text{ cm}^{-2}$, which is typical for warm absorbers. The column densities are plotted in Figure 3 with solid lines for C07 and dashed lines for C84. It is seen that the column densities of the major coolants changed significantly. The cooling agents are among the ions for which dielectronic recombination rate coefficients (hereafter DRRC) have been updated to the references below, as will be discussed in detail in Section 4. Thus the enhanced cooling in C07 due to the change in DRRC is the cause of the shift in the stability curves.

4 CHANGES IN DIELECTRONIC RECOMBINATION RATE COEFFICIENTS

The evolution of the thermal phases from the nebular temperatures of 10^4 K to the coronal temperatures of 10^6 K depends sensitively on the detailed atomic physics of the various elements which contribute to photoelectric heating as well as to cooling due to recombination and collisionally excited lines. In Table 2, we have compared the total recombination rates (dielectronic + radiative) for the significant cooling agents as predicted by C07 and C84. The val-

Ion	$\log T$	$\log \xi$	Recombination rates (s^{-1})	
			C07	C84
He^{+1}	5.34	2.00	1.66	-
Si^{+10}	"	"	1.36×10^{-1}	2.26×10^{-2}
Si^{+11}	"	"	8.85×10^{-2}	2.50×10^{-2}
Fe^{+21}	"	"	9.06×10^{-2}	2.20×10^{-2}
Fe^{+22}	"	"	8.36×10^{-2}	2.37×10^{-2}
Fe^{+23}	"	"	5.77×10^{-2}	2.28×10^{-2}

Table 2. Recombination rates of the dominant cooling agents obtained using C84 and C07. The ions are given in column 1. The temperature and ionization parameter at which the recombination rates have been obtained are noted in columns 2 and 3 respectively. The fourth and the fifth columns respectively give the value of the recombination rates predicted by C07 and C84.

ues for $\log T$ and $\log \xi$ at which the comparisons have been made are given in columns 2 and 3 respectively. For all the ions the total recombination rates are significantly higher in C07 than in C84 as

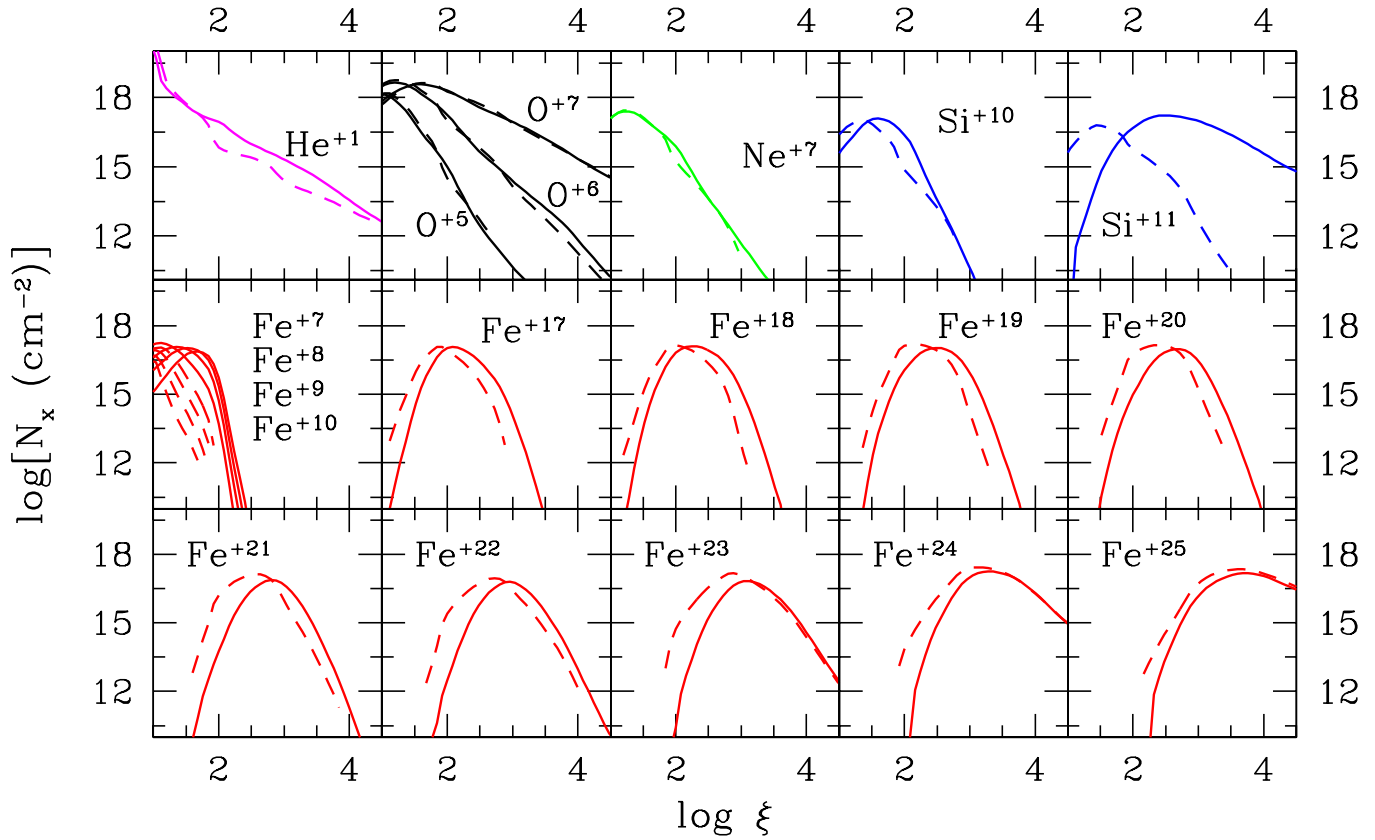


Figure 3. The column densities for the same ions as in the middle and bottom panel of Figure 2. The solid lines are predicted by C07 and the dashed lines are for C84. The difference in the column densities are more pronounced for the ions which are significant cooling agents, with Si^{+11} showing as much as a difference of about two orders of magnitude at $\log \xi \sim 2.0$ where it acts as the dominant cooling ion.

shown by columns 4 and 5. Referring to Figure 2, we see that the differences in total recombination rates are relatively larger for ions like Si^{+10} , Si^{+11} , Fe^{+21} and Fe^{+22} which are significant cooling agents for $\log \xi \sim 2.0$ and $\log \xi \sim 3.2$, corresponding to which we have maximum difference in predicted equilibrium temperatures T_{C07} and T_{C84} .

In the warm absorber temperature range $10^5 \lesssim T \lesssim 10^7$ K, dielectronic recombination dominates over radiative recombination for many ions (Osterbrock & Ferland, 2006). Unlike the radiative recombination rate coefficients, the DRRC have undergone significant changes over the last decade. C84 used DRRC from Nussbaumer & Storey (1983;1984; 1986; and 1987) and Arnaud & Raymond (1992). In C07 we have taken the DRRC for the isoelectronic sequences of lithium, beryllium, boron, carbon, nitrogen, oxygen and iron like ions respectively from Colgan et al. (2004), Colgan et al. (2003), Altun et al. (2004), Zatsarinny et al. (2004a), Mitnik & Badnell (2004), Zatsarinny et al. (2003), and Gu (2003). The DRRC for Ne to Na like ions and Na to Mg like ions are taken from Zatsarinny et al. (2004b) and Gu (2004). The C07 DRRC for any given ion is usually substantially larger than the C84 DRRC when the temperature is much lower than the ionization potential of the ion. The significant cooling agents in C07 are among these ions. This indicates that the updated DRRC database in C07 is the cause of the changes in the stability curve.

It is seen from Table 2 that the increase in recombination rates

from C84 to C07 is larger for the lower ionization species. The reason for the large increase, in general, in the low-temperature DRRC (referenced above) is the explicit inclusion of the contribution from low-lying (in energy) level-resolved dielectronic recombination resonances which have been accurately positioned by reference to the observed core energies. Unlike high-temperature dielectronic recombination, where the full Rydberg series contributes, low-temperature dielectronic recombination is not amenable to simple scaling or empirical formulae or guesses. Zatsarinny et al (2003) illustrate the radical and erratic changes in the low-temperature DRRC on moving between adjacent ions of the same isoelectronic sequence and, even, on changing from a term-resolved picture to level-resolved one for the same ion.

The DRRC database is still not complete, specially for the lower ionization states. For ions which do not have computed DRRC values, C07 uses a solution, as suggested by Ali et al. (1991); for any given kinetic temperature, ions that lack data are given DRRC values that are the averages of all ions with the same charge. The advantage of this method is that the assumed rates are within the range of existing published rates at the given kinetic temperature and hence cannot be drastically off. However we have checked whether the points in the C07 stability curves have computed DRRC values or guessed average values, concentrating on the parts of the curve which have multiphase solutions for the warm absorber ($10^5 \lesssim T \lesssim 10^6$ K) and are different from the C84 sta-

bility curve. We find that all the ions which act as major cooling agents for each of these points in the stability curve have reliable computed DRRC values. Thus, the new data base provides a more robust measurement of the various physical parameters involved in studying the thermal and ionization equilibrium of photoionised gas.

5 CONCLUSION

We have shown that stability curves for warm absorbers in AGN generated by two versions of the ionization code CLOUDY, C84 and C07, for the same physical conditions, are substantially different in shape, leading to different conclusions regarding the nature of the warm absorber. The differences in the results of the photoionisation calculations arise due to major changes in the dielectronic recombination rate coefficient (DRRC) data bases which have taken place over the last decade. The modern version C07 includes reliable computed DRRC values for many more ions than C84 for the entire part of the stability curve relevant for warm absorbers and does not rely on guessed average values. Thus, the physical nature of the warm absorber predicted by modern calculations are more reliable. We suggest that past calculations for photoionised plasma in thermal equilibrium should be reconsidered, taking into account these changes. Since, any other atomic physics code (eg. XSTAR), in popular use for warm absorber studies, is also likely to be affected by the changes in the DRRC data base, caution should be exercised while using or comparing results from them as well.

ACKNOWLEDGEMENTS

We thank Smita Mathur for reading an early version of the draft and providing helpful suggestions.

REFERENCES

- Ali, B. et al. 1991, *PASP*, 103, 1182
 Altun, Z. et al. 2004, *Astron. Astrophys.* 420, 775
 Arnaud, M., Raymond, J., 1992, *ApJ*, 398, 394
 Ashton, C. E. et al. 2006, *MNRAS*, 366, 521
 Colgan, J. et al. 2003, *Astron. Astrophys.* 412, 597
 Colgan, J., Pindzola, M.S. & Badnell, N.R. 2004, *Astron. Astrophys.* 417, 1183
 Collinge, M. J. et al. 2001, *ApJ*, 557, 2
 Ferland, G.J. et al. 1998, *PASP* 110, 761
 Gehrels, N & Williams, E.D. 1993, *ApJ* 418, L25
 Grevesse, N., & Anders, E. 1989, *Cosmic Abundances of Matter*, AIP Conference Proceedings 183, 1
 Grevesse, N. & Noels, A. 1993, *Origin & Evolution of the Elements*, Cambridge Univ. Press, p.15
 Gu, M. F. 2003, *ApJ*, 590, 1131
 Gu, M. F. 2004, *ApJS*, 153, 389
 Kaastra, J. S. et al. 2002, *A&A*, 386, 427
 Komossa & Mathur 2001, *A&A*, 374, 914
 Krolik, J., & Kriss, G. A. *ApJ* 561:684, (2001)
 Krolik, J. H., McKee, C. F., & Tarter, C. B. 1981, *ApJ*, 249, 422
 Krongold et al. 2003, *ApJ*, 597, 832
 Krongold et al. 2005, *ApJ*, 606, 151
 Mitnik, D.M. & Badnell, N.R. 2004, *Astron. Astrophys.* 425, 1153
 Morales, R., Fabian, A. C. & Reynolds, C. S. 2000, *MNRAS*, 315, 149
 Netzer, H. et al. 2003, *ApJ*, 599, 933
 Nussbaumer, H., & Storey, P. J. 1983, *A&A*, 126, 75
 Nussbaumer, H., & Storey, P. J. 1984, *A&AS*, 56, 293

- Nussbaumer, H., & Storey, P. J. 1986, *A&AS*, 64, 545
 Nussbaumer, H., & Storey, P. J. 1987, *A&AS*, 69, 123
 Osterbrock & Ferland 2006, *Astrophysics of Gaseous Nebulae and Active Galactic Nucleii*
 Reynolds, C.S. and Fabian, A.C. 1995, *MNRAS* 273:1167
 Tarter, C.B., Tucker, W. & Salpeter, E.E. 1969, *ApJ* 156:943
 Zatsarinny, O. et al. 2003, *Astron. Astrophys.* 412, 587
 Zatsarinny, O. et al. 2004a, *Astron. Astrophys.* 417, 1173
 Zatsarinny, O. et al. 2004b, *Astron. Astrophys.* 426, 699